Facies (2008) 54:597–612
DOI 10.1007/s10347-008-0145-5

ORIGINAL ARTICLE

Deposition within the vicinity of the Mid-Eifelian High: detailed sedimentological study and magnetic susceptibility of a mixed ramp-related system from the Eifelian Lauch and Nohn formations (Devonian; Ohlesberg, Eifel, Germany)

Cédric Mabille · Damien Pas · Markus Aretz · Frédéric Boulvain · Stephan Schröder · Anne-Christine da Silva

Received: 24 September 2007 / Accepted: 18 April 2008 / Published online: 17 May 2008

Abstract This study focuses on the base of the Eifelian stage and on the abandoned Ohlesberg quarry. The exposed section (92 m thick) is related to the Lauch and Nohn formations. Petrographic study leads to the definition of 11 microfacies which are integrated in a palaeogeographical model. It corresponds to a complex ramp setting where carbonate, mixed and siliciclastic deposits coexist. The microfacies evolution is interpreted in terms of bathymetric and lateral variations, showing a general shallowing-upward trend and transitions between carbonate-dominated and siliciclastic-dominated sedimentary domains. This interpretation is supported by trends in magnetic susceptibility data. Even if the proximity to emerged areas appears to be the major influence on magnetic susceptibility values, the influence of carbonate productivity and wave agitation is also noted. The Ohlesberg section clearly points to the local and regional complex facies architecture, and advocates to variegated depositional environments along the Mid-Eifelian High.

Keywords Middle Devonian · Type Eifelian · Sedimentology · Sötenich Syncline

C. Mabille (✉) · D. Pas · F. Boulvain · A.-C. da Silva
Pétrologie sédimentaire, B20, Université de Liège,
Sart-Tilman 4000, Liège, Belgium
e-mail: cmabille@ulg.ac.be

D. Pas
e-mail: damienPas@hotmail.com

F. Boulvain
e-mail: fboulvain@ulg.ac.be

A.-C. da Silva
e-mail: ac.dasilva@ulg.ac.be

M. Aretz · S. Schröder
Institut für Geologie und Mineralogie, Universität zu Köln,
Zülpicher Str. 49a, 50674 Cologne, Germany
e-mail: markus.aretz@uni-koln.de

S. Schröder
e-mail: ste.schroeder@gmx.net

Introduction

The Eifelian in its type area, the Eifel Synclines (Eifeler Kalkmulden Zone), is world famous for the abundance of fossils, intensively studied for more than 200 years (e.g., Goldfuss 1826; Steiniger 1853; Schlüter 1889). Mapping and stratigraphical studies of the "Frankfurt School" of the 1950s and 1960s (e.g., Krömmelbein et al. 1955; Paulus 1959, 1961; Ochs and Wolfart 1961; Glinski 1961) resulted in a very detailed stratigraphical subdivision of the Eifelian succession. This is highlighted by the proposition of standardised stratigraphic units, the so-called "type-Eifelian" (Struve 1982) based on the succession of the Hillesheim Syncline.

Compared to abundant palaeontological and biostratigraphical studies, sedimentology and facies are surprisingly poorly studied in the Eifelian type area. Earlier, others (e.g., Happel and Reuling 1937; Nowak 1956; Ochs and Wolfart 1961; Struve 1963) had noted important spatial and temporal facies variations, but at that time the problem had often been reduced to the significance of local stratigraphic units that did not fit into the standardised succession (e.g., Paulus 1959, 1961).

Subsequent facies studies (Winter 1977; Faber 1980) resulted in the recognition of three major facies realms. The general facies pattern (Fig. 1) differentiates (A) a northern realm in a more proximal shelf position with important influx of coarser siliciclastics from the northern emerged

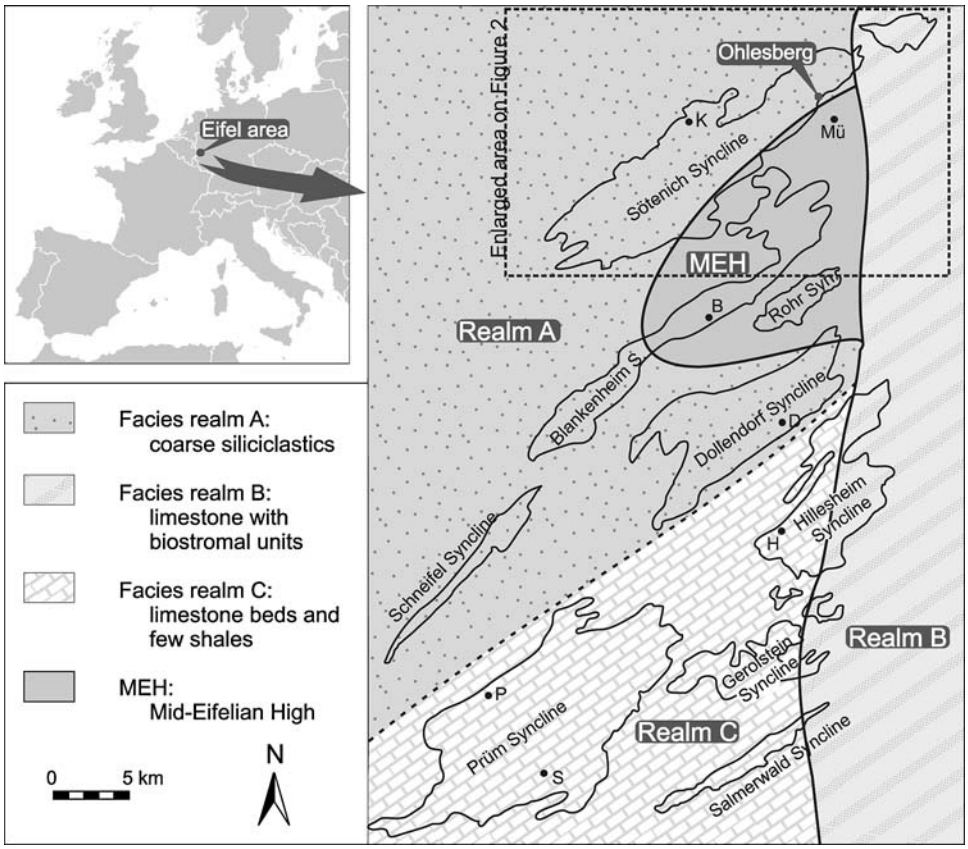

Fig. 1 General facies model for the Eifelian of the Eifel Synclines (modified from Faber 1980) showing facies realms: *realm A* is in a more proximal shelf position with important influx of coarser siliciclastics from the northern emerged areas; *realm B* shows the repeated development of a carbonate platform system; and *realm C* is characterised by limestone beds and minor shales in more distal position. *B* Blankenheim; *D* Dollendorf; *H* Hillesheim; *K* Kall; *Mü* Bad Münstereifel; *P* Prüm; *S* Schönecken; *MEH* Mid-Eifelian High

areas, (B) an eastern realm showing the repeated development of carbonate platform systems in variable size through time, and (C) a southern realm in a more distal position characterised by limestone beds and minor shales. However, topographic irregularities may significantly modify this general picture. This facies model also explained that the application of the detailed type-Eifelian stratigraphic subdivision is almost impossible for the entire Eifel Synclines, especially since the succession of the Hillesheim Syncline represents several stages of different local carbonate platforms (Faber 1980). Thus, throughout the entire Eifel Synclines individual isochrones are characterised by faunal and lithological differences and not by uniform facies or faunas. Rehfeld (1986) stated that the differentiation into numerous very short stratigraphic units (horizons and sets of Struve) hampers the interpretation of the general picture, and also indicates the importance of the facies variability.

One of the important intra-depositional highs is the Mid-Eifelian High (MEH in Fig. 1), which comprises the central and eastern Blankenheim Syncline, the Rohr Syncline, and parts of the north-eastern Sötenich Syncline. It is clearly visible in the sigmodial shape of the facies belts in the palaeogeographic reconstructions of Struve (1963) and Faber (1980). However, considerable variations in size and position of the high and resulting facies distribution shall be envisaged for individual time slices as already stated by Struve (1963).

The Sötenich Syncline (Fig. 2) is the most northern and one of the largest synclines within the Eifel Synclines. It comprises a thick Middle Devonian succession, but widespread dolomitisation and a thrust crossing the entire syncline almost parallel to strike hampers the recognition of Upper Devonian strata as in the Prüm Syncline. In comparison to the other Eifel Synlines, the Sötenich Syncline is positioned most proximal to the Old-Red Continent. It is thus much more affected by clastic influx than the other synclines, and Eifelian lithologies may often be similar to Lower Devonian strata (reddish colours). Nowak (1956) studied the NE part of the Sötenich Syncline, and the Ohlesberg is situated in the SW corner of his mapping area. The middle part of the syncline was mapped by Paulus (1959, 1961), the south–eastern by Dickfeld (1969). In all three areas, local stratigraphic units have been introduced due to facies changes and/or few biostratigraphical reliable fossils (Fig. 3).

Concerning the Nohn Formation, Nowak (1956) already recorded locally difficult outcrop conditions, but he could show variations in thickness and facies. The general development of stromatoporoid–coral facies at the base (with exception of the Eschweiler area) is followed by a phase of differentiation into *Thamnopora* and stromatoporoid reef facies. In some areas, siliciclastic input hampers carbonate production. In the upper part of the formation, sandstones

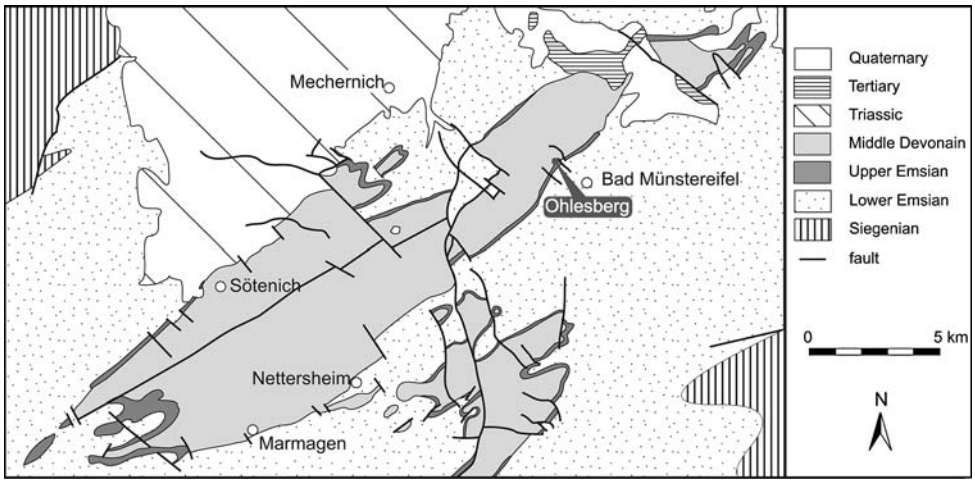

Fig. 2 Localisation of the Ohlesberg on simplified geological map of the Sötenich Syncline and adjacent structural units (from Meyer 1994)

	Formation	Type-Eifelian			NE Söt. Syncline		Central Söt. Syncline	
		Subform.		*Member*			*North*	*South*
EIFELIUM	AHBACH				*Lithostratigraphic units*			
	FREILINGEN							
	JUNKERBERG							
	AHRDORF							
	NOHN	Stroheich		Hundsdell	N4: Hundsdell	Studied interval	Hundsdell	
				Dankerath	N3: calcareous sandstones		Dankerath	
		Zilsdorf	Ahütte	Hunnertsberg	N2: *Thamnopora* and crinoidal lmst.		Schellgesberg	Lierberg
				Erdel				
				Markstein				
				Schmitzbach				
			Kirberg	Schleit	N1: Stromatoporid marls and lmst.		Urft	Eigen
				Weilersbach				
	LAUCH			Wolfenbach	L4: sandstone		Eulenkopf	
					L3: upper shales			
				Dorsel	L2: *Alatiformis* crinoidal lmst.		Weinberg	
					L1: lower shales			
EMS.	HEISDORF							

Fig. 3 Overview on the lithostratigraphic units of the Central (Nowak 1956) and NE (Paulus 1959, 1961; Dickfeld 1969) Sötenich Syncline and the type Eifelian nomenclature (Struve 1982)

spread out, but a carbonate shoal separates a western from an eastern area. In the uppermost part of the Nohn Formation, crinoidal limestones (Hundsdell Member) are recorded from most parts of the area. Confirmation of theses observations is today almost impossible as a consequence of the low number of Nohn exposures in the NE part of the Sötenich Syncline.

One remarkable exception to this lack of Nohn exposures is the abandoned Ohlesberg quarry (Fig. 4), which exposes at its base the upper Lauch Formation. The majority of the quarry succession comprises the Nohn Formation, and the topmost beds belong to the Ahrdorf Formation. The Ohlesberg quarry is situated on the southern limb of the north-eastern Sötenich Syncline, approximately 2 km NW of Bad Münstereifel (Fig. 2). Nowak (1956) described the complex tectonic deformation of the Ohlesberg, today still visible at the side of the access road. A brief description of the succession and information on microfacies and conodonts was given by Klein et al. (1998).

Aims of the study

From a regional point of view, it is the aim of this study (1) to describe the succession of the Lower Eifelian in the vicinity of the Mid-Eifelian High, and (2) to evaluate the

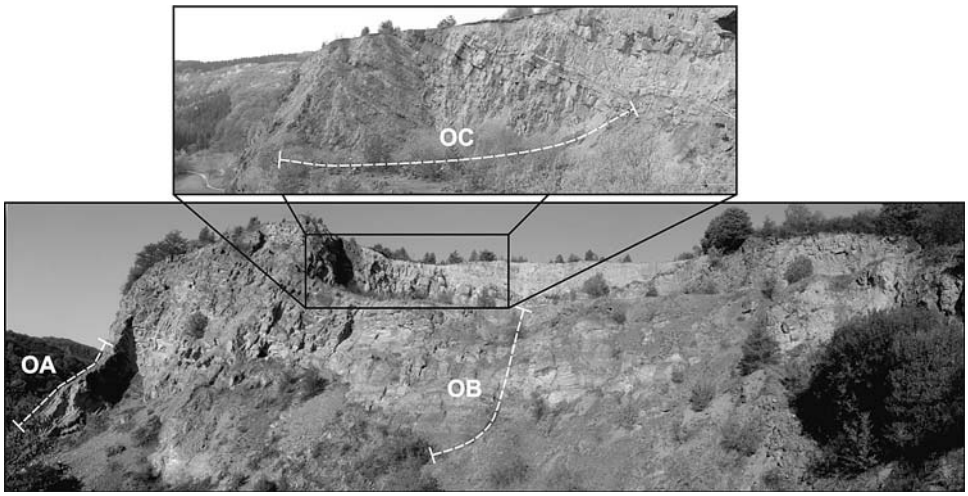

Fig. 4 The Ohlesberg Quarry showing position of *OA*, *OB* and *OC* subsections. View from the south

potential of a single locality to contribute to remaining open questions for a conclusive regional depositional model for the Eifel synclines. Thus, a detailed sedimentological and magnetic susceptibility study accompanied by data on corals and stromatoporoids has been conducted for the Lower Eifelian succession of the abandoned Ohlesberg quarry (NE Sötenich Syncline) positioned next to the Mid-Eifelian High (see Winter 1977).

Concerning Magnetic susceptibility (MS), the Ohlesberg section offers the opportunity to test this method introduced to Palaeozoic rocks during the 1990s (Hladil 1992; Crick et al. 1994, 1997, 2000; Ellwood et al. 2000). In fact, MS of sedimentary rocks, which is a measurement of the sample response to an external magnetic field, is regarded as mainly influenced by the terrestrial fraction (Ellwood et al. 2000). To test this link is of crucial importance because it is the basis for the use of MS as a correlative tool (Crick et al. 1997; Hladil 2002; da Silva and Boulvain 2006). High MS values are considered to be the result of increased siliciclastic inputs into the sedimentary basin. This is interpreted to be linked to eustasy because the erosion of exposed continental masses increases during sea-level falls. However, on the contrary, when the sea level rises, MS shows lower values. This relatively simplified vision of MS variations caused only by eustasy is complicated by other parameters like climatic changes (precipitation, ice ages, pedogenesis), tectonism, diagenesis, volcanism and impact ejecta (Crick et al. 1994; Ellwood et al. 1999; Stage 2001). Moreover, MS measurements of Middle Devonian sections of Belgium recently showed that wave agitation is, in combination with terrigenous input, a main influencing parameter possibly responsible for non-deposition of MS carrying minerals (Mabille and Boulvain 2007a, b, 2008). The role of carbonate productivity and sedimentation rate has also been considered to lower MS signal by diluting MS carrying minerals (da Silva et al. 2008). In order to track these influencing parameters within the Ohlesberg quarry, a combination of facies analysis of carbonated-dominated and siliciclastic-dominated facies and their magnetic properties is implemented here.

Methods

A bed-by-bed description and sampling was carried out, and 200 thin-sections were prepared. The textural classification used to characterise the microfacies follows Dunham (1962) and Embry and Klovan (1972). The description of stromatoporoids is based on the morphological classification of Kershaw (1998); herein the terms branching, laminar, domical and bulbous are used. Massive is used for both domical and bulbous forms (Tucker and Wright 1990) when the difference cannot be detected (fragments or thin-sections). Estimation of sorting is based on the visual charts of Pettijohn et al. (1972).

Thin-section analyses have lead to the definition of 11 major microfacies types and four microfacies subtypes. Interpretation of each microfacies is based on (1) relative positions to fair-weather and storm-wave bases, even if water depths of these boundaries may vary in relation to local hydrodynamic or climatic conditions (Burchette and Wright 1992), and on (2) lateral variations between carbonate-dominated and siliciclastic-dominated sedimentary domains, some microfacies types corresponding to lateral equivalents with various terrigenous influence. Combination of these interpretations allows the reconstruction of a three-dimensional sedimentological model, and plots of microfacies trends.

The magnetic susceptibility of each sample was measured three times with a KLY-3 (Kappabridge) and weighed with a precision of 0.01 g. These measurements allow the definition of the mass-calibrated magnetic susceptibility of each sample and the construction of magnetic susceptibility plots.

Results

Description of section

The outlet of the quarry does not allow measurement of a single continuous log from the base of the quarry to its top. Thus, the description is based on a composite log of three sections respectively called OA, OB, and OC (see Fig. 4 for location within the quarry). These sections are in stratigraphical order and allow the study of an almost continuous succession of strata. The stratigraphic gap between OA and OB is estimated at 2 m and at 3 m between OB and OC. The composite section is 92 m thick (Fig. 5a).

The section starts with 10 m of variegated calcareous sandstone and sandy limestones corresponding to the topmost part of the Lauch Formation. Some beds show laminations corresponding to bioclastic fining-upward levels. The fauna is relatively poor (low diversity and abundance) with only some crinoids, brachiopods (*Altiformia* sp.), solitary rugose corals (*Mesophyllum* (*Mesophyllum*) sp., *Acanthophyllum* sp.), and tabulate corals (*Alveolites intermixtus*). Few massive stromatoporoids, up to 30 cm in diameter, are observed at the top of the unit, where also corals become somewhat more abundant.

The lower part of the Nohn Formation begins with the vertical succession of three units from 10 to 19 m (numbered i, ii and iii on Fig. 6j).

1. The first 3 m correspond to *Cladopora*-enriched marls. Laminar and massive stromatoporoids, massive tabulate corals (*Favosites*), and few colonial rugose corals (*Sociophyllum*, *Battersbyia*) are also observed. All laminar and branching organisms are fragmented (<10 cm) and deposited parallel to bedding.
2. The second one (next 2 m of section) is characterised by the same kind of *Cladopora*-enriched marls interbedded with more calcareous and consolidated lenses (10 cm to 1 m in length and 5–50 cm in thickness). These lenses become more abundant and thicker from the base to the top. The fauna is similar to unit 1 but differs by the occurrence of fasciculate rugose corals and by the presence of in situ domical stromatoporoids (up to 40 cm in diameter).
3. The last unit corresponds to an accumulation of laminar and massive stromatoporoids. These organisms are mostly found in living position and can reach more than 1 m in width and 50 cm in height. Between these organisms, more argillaceous and bioclastic lenses with crinoids, tabulate corals (*Heliolites porosus lindstroemi*, *Caunopora*), thin laminar stromatoporoids, and solitary rugose corals (*Mesophyllum* (*Mesophyllum*) are observed.

From 19 to 37 m, the section consists of partly bituminous thin-bedded limestone. In the upper third, the limestone becomes more marly and sandy. Some shaly interbeds are also present. The fauna is abundant and represented by crinoid debris, brachiopods, ostracods, gastropods and corals (*Thamnopora*, *Dendrostella*, *Mesophyllum*).

From 37 to 54 m, the section is composed of marl, siltstone, and various marly limestone. The faunal assemblage is more diversified with abundant branching tabulate corals, crinoids and brachiopods. The occurrence of solitary rugose corals, massive and laminar stromatoporoids, and huge in-situ colonies (up to 1.5 m in diameter) of fasciculate rugose corals (*Mesophyllum*) is also noted. The occurrence of *Mesophyllum (Mesophyllum) vesiculosum vesiculosum* (Goldfuss 1826) is most striking, as the stratigraphical age of most records was restricted to the Lower Givetian (Birenheide 1978). Only recently a few specimens were recorded from Upper Eifelian strata of the Dollendorf Syncline (Schröder 1998), but none of the records reached the base of the Eifelian. Such an extension in stratigraphical range is most unusual, but the Ohlesberg specimens are very similar and are most likely conspecific.

The following part of the section (from 54 to 85 m) corresponds to the Dankerath Member of the upper Nohn Formation. It is characterised by thick beds of sandstone and argillaceous siltstone. Few bioclastic-rich and calcareous sandstone beds and shaly interbeds are also present. The dominating colour of these rocks is green and grey (in the lower quarter of the member), then red (in the following quarter), and grey again (in the upper half). Bioturbation occurs locally throughout the entire member. Sandstone beds often show sedimentary structures like planar bedding, cross bedding, and oscillation ripple marks. Most beds are free of fossils but some contains crinoid debris, brachiopods, and terrestrial plant debris. The ichnofossil *Lennea schmidti* is locally abundant.

The top of the section (from 85 to 92 m) belongs to the Hundsdell Member and corresponds to slightly reddish pure limestone (beds between 10 and 50 cm) alternating with 1-cm-thick red shale beds. The (macro) fauna is abundant in the limestone beds but consists only of crinoid debris and brachiopods. All fossils are red coloured by iron oxides. Two mottled nodular argillaceous beds (respectively 30 cm and 1.20 m thick) corresponding to palaeosoils are also observed (see microfacies interpretation for more details). The boundary to the Ahrdorf Formation was not crossed in this study, but according to the data of Klein et al. (1998), it follows up-section.

Description and interpretation of microfacies types

Microfacies types are described from the most distal to the most proximal ones and are illustrated in Fig. 6 and in the synthetic model Fig. 7.

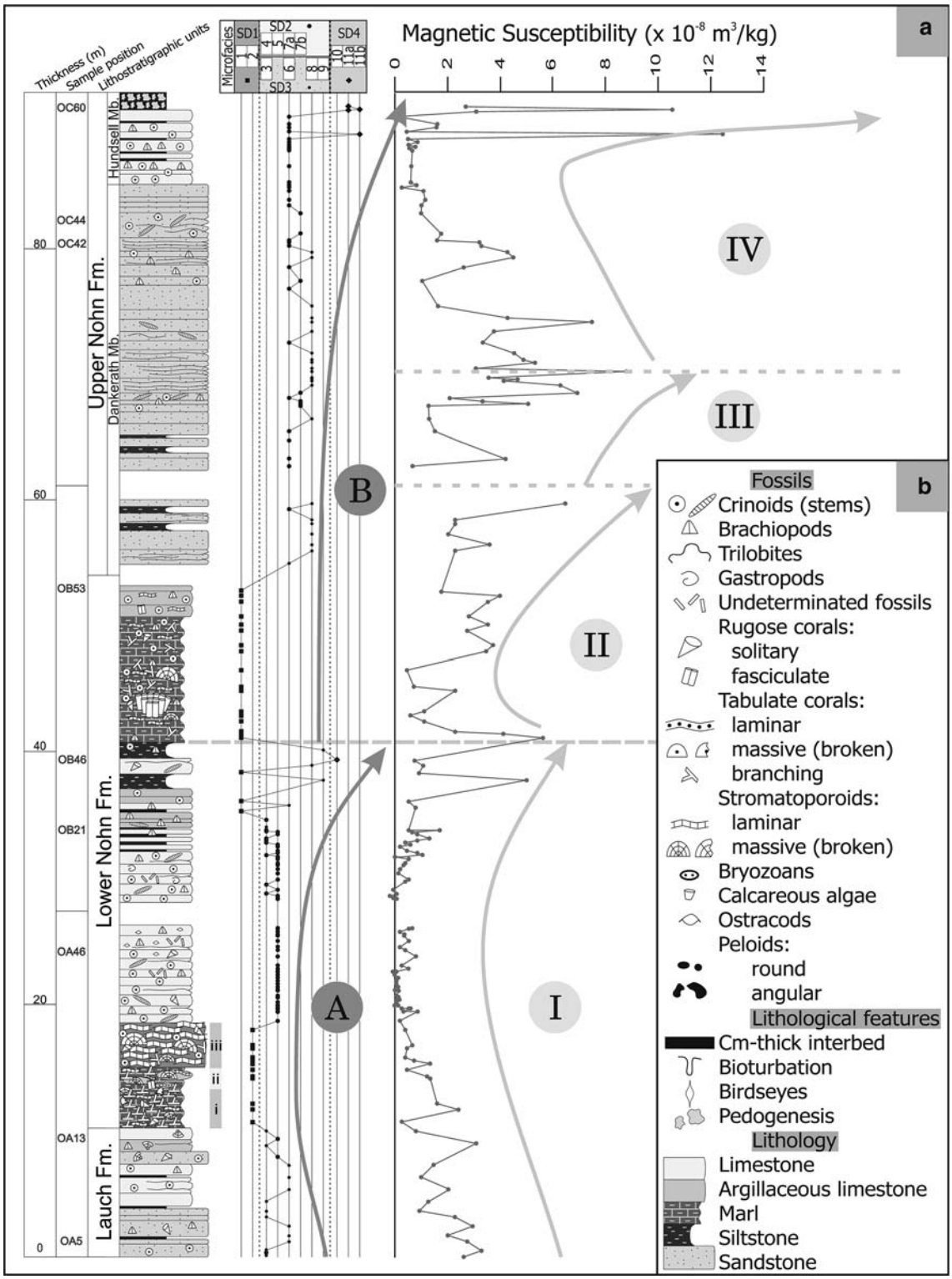

Fig. 5 **a** Schematic sedimentological log, lithostratigraphic units (*Fm.* formation; *Mb.* member), microfacies trends, and magnetic susceptibility curves. *Arrows* represent trends in facies (*A* and *B*) and magnetic susceptibility (*I–IV*) evolution. **b** Legend for symbols used in figures

MFO1: crinoid–coral-floatstone

Between debris (ranging from 0.5 to 5 cm) of branching tabulate corals, solitary and fasciculate rugose corals, and laminar stromatoporoids, the matrix (packstone texture) is composed of often rounded crinoids, brachiopods, tentaculitids, trilobites, ostracods, and bryozoans (Fig. 6a). Dasycladaceans, *Girvanella*, and *Asphaltina* are observed.

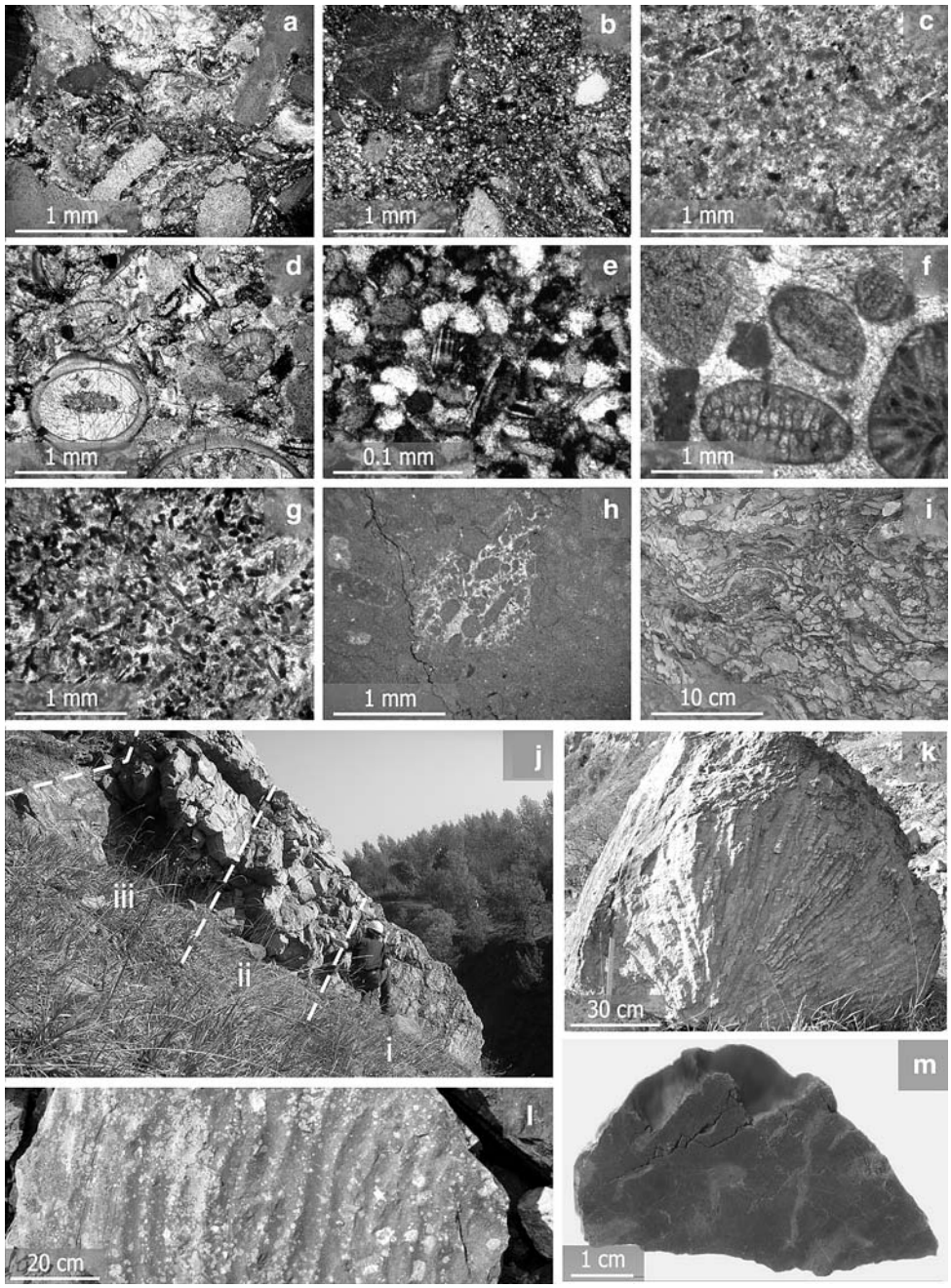

Fig. 6 Facies of the Ohlesberg section. *Numbers in brackets* correspond to bed numbers on Fig. 5a. See text for more explanations: **a** MFO1: bioclastic floatstone with crinoids and tabulate coral in a silty-argillaceous matrix (OB53), thin-section, normal light. **b** MFO3: crinoidal sandstone (OA13), thin-section, normal light, alizarine stain. **c** MFO4: peloidal grainstone (OB21), thin-section, normal light. **d** MFO5: crinoidal grainstone with tentaculitids and dasycladaceans (OA46), thin-section, normal light. **e** MFO6: calcareous sandstone with plagioclase grains and mica sheets (OA5), thin-section, crossed nicols. **f** MFO7a: hematitized grainstone with abundant crinoids and few peloids showing branching bryozoans (OC42), thin-section, normal light. **g** MFO7b: grainstone with hematitized peloids (OC44), thin-section, normal light. **h** MFO10: wackestone with a bioturbation filled by a peloidal matrix (OB46), thin-section, normal light. **i** MFO2: bioclastic marl with branching tabulate corals and laminar stromatoporoids. **j** Units *i, ii* and *iii* observed at the base of the lower Nohn Formation (OA subsection). **k** MFO1: large colony of *Mesophyllum* (erratic block). **l** MFO8: ripple marks (erratic block). **m** MFO11b: mottled claystone (OC60)

Asymmetrical encrusting by calcareous algae, bryozoans and tabulate corals are present around some branching tabulate corals, solitary and fasciculate rugose corals and laminar stromatoporoids. This microfacies is associated with huge colonies of *Mesophyllum* (Fig. 6k) preserved in living position. Detritic quartz (from 0.01 to 0.1 mm) content is 10–20% for most samples but locally reaches 40–50%. This silty-argillaceous matrix also contains mica sheets (up to 2.5%) and plagioclase (<1%), and can be affected by dolomitisation.

Interpretation. The presence of clay between bioclasts indicates accumulation of suspended mud (Flügel 2004). The low sedimentation rate in a quiet environment is confirmed by the presence of in situ colonies of *Mesophyllum*. However, the abundance of bioclasts within packstone could indicate more energetic periods. This may correspond to a concentration of bioclasts via storm action removing part of the matrix. Thus, this microfacies is located between the fair-weather wave base (FWWB) and the storm-wave base (SWB). The faunal and algal assemblages indicate fully marine conditions. Local abundance of debris of tabulate corals, rugose corals, and few laminar stromatoporoids indicates the close proximity of bioconstructed facies (corresponding to MFO2). Moreover, matrices from MFO1 and

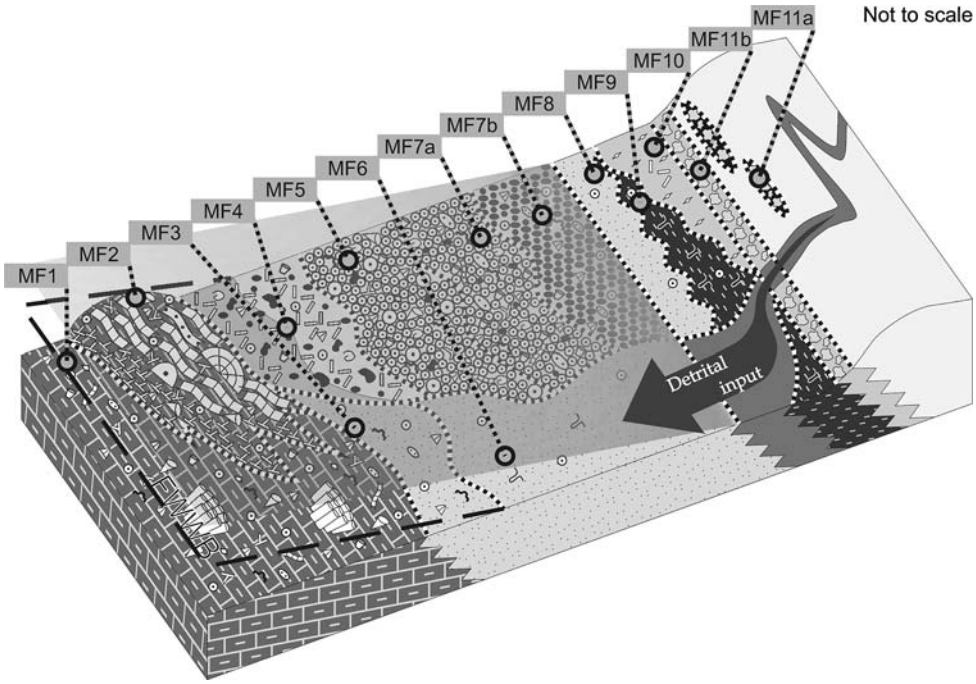

Fig. 7 Proposed palaeoenvironmental model (see Fig. 5b for legend) corresponding to a complex ramp profile where carbonated, mixed and siliciclastic deposits coexist

MFO2 are similar confirming the vicinity of these two microfacies types.

MFO2: coral–stromatoporoid-rudstone

Branching tabulate corals and laminar stromatoporoids (up to 1 m in diameter) dominate this rudstone (Fig. 6i). Other organisms are laminar and massive tabulate corals, massive stromatoporoids, and solitary rugose corals. Massive and laminar forms are occasionally found in living position, but the majority is reworked. Between these large organisms, smaller bioclasts (from 0.5 mm to 2 cm) are observed, like crinoids and brachiopods. Some bryozoans, trilobites, pelecypods, ostracods, tentaculitids, gastropods, and dasycladacean algae are also present. Some of them are perforated. Encrusting stromatoporoids and bryozoans are observed around some solitary rugose corals and gastropods. The argillaceous matrix is intensely dolomitised and locally contains detrital quartz (from 0.01 to 0.1 mm and up to 2.5%) and mica sheets (<1%).

Interpretation. The presence of abundant, broken branching tabulate corals within an argillaceous matrix indicates quiet periods of mud deposition and growth of corals interrupted by energetic events such as storms, responsible for the reworking of corals. MFO2 corresponds to a fully marine environment (indicated by the presence of brachiopods, trilobites, and tentaculitids) located between FWWB and SWB. Moreover, this microfacies is found at the base of the lower Nohn Formation, and corresponds to the substrate of large laminar stromatoporoids found in the overlying unit (see Fig. 6j: unit iii). Such a development of stromatoporoids corresponds to favourable conditions in terms of bathymetry (in link with plausible phototropism), substrate and sufficiently low detrital input (Kershaw 1998). In this context, laminar stromatoporoids indicate poorly stabilised substrate or low sedimentation rate (Kershaw and Brunton 1999; corresponding here to an argillaceous matrix).

MFO3: partly laminated bioclastic sandstone

Detrital quartz is dominant with concentrations up to 60%. Grains, from 0.01 to 0.1 mm, are poorly rounded with poor sphericity. Angular grains of plagioclase (from 0.05 to 0.15 mm), mica sheets and clays are concentrated in lenses. Bioclasts (from 0.2 to 4 mm) are dominated by crinoids but brachiopods, tentaculitids, trilobites, bryozoans, pelecypods, and *Girvanella* are also present. In most cases, a mixture of siliciclastic material and bioclasts is observed (Fig. 6b) but slight lamination can be locally preserved: bioclastic rich grainstone layers alternate with layers rich in quartz. These laminations are 0.4–8 mm thick. The cement of these grainstone layers is an equigranular sparite.

Interpretation. The alternation of clay and coarser grained sediments suggests only temporary agitation. However, the dominance of bioclastic sandstone versus clay layers indicates very proximal storm deposits (Aigner and Reineck 1982). This corresponds in fact to the amalgamation of storm deposits with erosion of the major part of a classical storm sequence (see, e.g., Howard and Reineck 1981). This led to the preservation and repetition of truncated sequences, mainly corresponding to the coarser

material deposited at the base of the sequence. The presence of these amalgamated storm deposits coupled with the local presence of lamination indicates a position within the shoreface to transition zone (sensu Aigner and Reineck 1982). The environment is both influenced by fully marine conditions with crinoids, brachiopods, tentaculitids, and bryozoans, and by an important terrigenous input (quartz, plagioclase, mica sheets, and clay). These imply a location just below FWWB but above SWB with an important terrigenous influence.

MFO4: peloidal packstone and grainstone

This microfacies type is characterised by (1) the presence of poorly preserved and often undeterminable bioclasts (mostly ranging from 0.1 to 0.5 mm) and by (2) the presence of 20–40% of peloids (Fig. 6c). Two different types of peloids are observed. Most frequent are ovoidal to spherical peloids ranging from 0.1 to 0.2 mm in diameter. The second type corresponds to larger (up to 0.4 mm) and irregular-shaped peloids (showing local preservation of relics of bioclasts). Determinable bioclasts (generally between 0.1 and 0.5 mm) are uncommon: brachiopods, crinoids, tentaculitids, gastropods, and dasycladaceans. The sorting is relatively good. Packstones are characterised by a micritic matrix containing up to 5% of detrital quartz and are locally argillaceous or dolomitised. Grainstone cement is mostly an equigranular sparite (locally dolomitised) even if some crinoids are surrounded by syntaxic cement.

Interpretation. The main characteristic of MFO4 is the abundance of peloids. Origins of peloids can be diverse: faecal, micritised grains, direct algal origin, and intraclasts (Tucker and Wright 1990). Even if the micritisation of bioclasts is proven by the local preservation of relics within larger peloids, other origins cannot be excluded. Bioclasts advocate for fully marine conditions (brachiopods, crinoids, tentaculitids). Relatively good sorting and grainstone texture without any sedimentary structure suggest a location above the FWWB (Wright and Burchette 1996). However, the regular occurrence of packstones and clay indicates quiet periods, finally pointing to a location around the FWWB.

MFO5: crinoidal grainstone

This grainstone is dominated by crinoids (Fig. 6d) representing up to 90% of the allochems. Crinoid grains mostly range from 0.2 to 1 mm even if some reach up to 2 cm in diameter. The rest of the allochems are brachiopods, tentaculitids, gastropods, trilobites, and more uncommon pelecypods, ostracods, dasycladaceans, and *Girvanella*. Most of them are broken and measure less than 1 mm. Exceptions include some brachiopods (up to 1 cm), entire gastropods (up to 4 mm), dasycladaceans (from 2 to 3 mm) and tentaculitids (up to 3 mm). Peloids (irregular in shape, from 0.1 to 0.3 mm) and intensively broken debris of branching tabulate corals, solitary rugose corals and laminar stromatoporoids are locally observed. The sorting is bimodal, with larger and better-preserved millimetric organisms mixed with smaller and poorly preserved ones (around 0.5 mm). Detrital quartz and mica sheets are uncommon (<1%). The cement is an equigranular sparite (locally dolomitised), and some crinoids are surrounded by syntaxic cement.

Interpretation. MFO5 corresponds to the dismantling of crinoidal meadows just above the FWWB (Préat and Kasimi 1995). Brachiopods, trilobites, and tentaculitids indicate fully marine setting.

MFO6: calcareous sandstone

Detrital quartz is dominant with concentrations up to 80%. Quartz grains, from 0.01 to 0.1 mm, are poorly rounded with an intermediate sphericity. Angular grains of plagioclase (from 0.05 to 0.15 mm) and mica sheets are also present (Fig. 6e). Bioclasts (0.2–0.4 mm) are uncommon and intensively broken: crinoids, brachiopods, and trilobites. Some horizontal burrows with more argillaceous filling are locally observed. The cement is an equigranular sparite.

Interpretation. This microfacies is characterised by an important detrital content of quartz, plagioclase, and mica sheets. The absence of clay suggests a permanent agitation, inhibiting the deposition of small particles (Kumar and Sanders 1976). The absence of sedimentary structure is regarded as the result of intense bioturbation (Sepkoski et al. 1991). This would imply a position above FWWB. The poor faunal assemblage (crinoids, brachiopods and trilobites) indicates a fully marine influence.

MFO7a: coarse bioclastic grainstone

Hematitized bioclasts (from 1 mm to 1.5 cm) dominate the assemblage, whereas peloids represent less than 10%. Two other characteristics have to be noted: presence of branching bryozoans and *Asphaltina*. Bioclasts are well preserved (Fig. 6f) and are represented by crinoids, gastropods, brachiopods, trilobites, tentaculitids, *Girvanella*, and uncommon debris of branching and laminar tabulate corals and laminar stromatoporoids. These fossils are frequently encrusted by calcareous algae (mainly irregular encrustations) or bryozoans. Mud-coated grains are also observed. Detrital quartz is present (<5%). The cement is an equigranular sparite with local occurrence of syntaxic cement. Hematitisation concerns crinoids, peloids, and algal encrusting.

Interpretation. This grainstone is particularly coarse with poorly broken bioclasts. The absence of thin bioclasts

and detrital material suggests a high degree of agitation. Mud-coated grains characterise zones of permanent agitation and are associated with washed shoals in an internal ramp setting (Flügel 2004). A rapid burial, preventing against breaking by wave agitation, could explain the relatively good preservation of bioclasts. These imply a location above the FWWB.

MFO7b: peloidal grainstone

Hematitized peloids (around 0.2 mm) in this subtype are more abundant compared to MFO7a (20–90%; Fig. 6g). Bioclasts (around 1 mm) are less abundant and intensively broken: crinoids, brachiopods, bryozoans, trilobites, and few tentaculitids, *Girvanella*, and dasycladaceans. Mud-coated grains are still present but *Asphaltina* and branching bryozoans are uncommon. Detrital quartz is present and reaches concentrations of up to 5%.

Interpretation. Broken organisms indicate an intense reworking before burial. This is due to a less important sedimentation rate in comparison with MFO7a, allowing a longer exposure of bioclasts to wave agitation but also probably to biodegradation and biocorrosion. The more effective agitation coupled with the abundance of peloids indicates more proximal settings than in MFO7a (Tucker and Wright 1990). MFO7b is thus located above the FWWB.

MFO8: laminated micaceous sandstone

Detrital quartz is dominant (at least 70%). Grains, from 0.01 to 0.3 mm, are poorly rounded with an intermediate sphericity. Mica sheets and plagioclase are also observed. The lamination (0.2–0.4 mm thick) is underlined by light levels (dominated by quartz and plagioclase) alternating with darker ones (mica sheets, disseminated hematite, and eventually clay). This mainly corresponds to planar lamination but oscillation cross-bedding is locally observed. Ripple marks (Fig. 6l) and terrestrial plant debris are also observed. Bioclasts are uncommon and only represented by intensively broken crinoids.

Interpretation. The sedimentary structures correspond to shallow-water settings affected by wave oscillations (Johnson and Baldwin 1996). The proximity of emerged areas is confirmed by the presence of terrestrial plant debris.

MFO9: calcareous siltstone

Detrital quartz is dominant with concentrations of up to 80%. Grains, from 0.01 to 0.05 mm, are poorly rounded with an intermediate sphericity. Mica sheets and clays are also present. Horizontal and vertical burrows with more argillaceous filling are observed. However, thin planar lamination is locally observed (around 0.1 mm). It corresponds to dark levels enriched in clays and micas alternating with light levels richer in quartz. Crinoids are uncommon and intensively broken. The cement is an equigranular sparite.

Interpretation. This particularly fine-grained microfacies indicates a low energy setting where the main sedimentary process is the deposition of mud. Such environments are found in fully marine locations above the SWB or in internal protected settings (Préat and Kasimi 1995). The second hypothesis is preferred because of the poor faunal assemblage (Flügel 2004).

MFO10: fenestral wackestone with lithoclasts and poor fauna

Lithoclasts are various in form (rounded to angular) and in size (from 0.05 to 2 mm). They show a micritic texture. Bioturbations and fenestrae (from 1 to 2 mm) are filled with peloids (Fig. 6h) corresponding to "clotted structure" (Monty 1967). Fauna is particularly uncommon and only represented by completely recrystallised and intensively broken shells (around 0.4 mm). Detrital quartz and mica sheets are present. The matrix is a dark micrite.

Interpretation. Angular fenestrae filled with peloids or "clotted structure" are related to algal mats (Tucker and Wright 1990). These mats develop in upper intertidal to supratidal settings (Flügel 2004).

MFO11: palaeosoils

This microfacies type comprises limestone and claystone, which contain characterising pedogenesis processes.

MFO11a: nodular limestone

At the outcrop scale, this microfacies corresponds to nodular beds of limestone associated with desiccation cracks filled by red claystone. These nodules are composed of lithoclastic wackestone with ostracods, pelecypods, trilobites, brachiopods, palaeosiphonocladalean algae, solitary rugose corals, and completely recrystallised shells. This wackestone locally contains detrital quartz (up to 2%) and mica sheets. The matrix of the nodules is a locally argillaceous micrite. Some vertical cracks filled by an equigranular sparite are also observed.

Interpretation. Nodular beds can be related to the irregular secondary precipitation of carbonate in soils (Wright 1994) and vertical cracks indicate seasonal cycles of retraction (dry season) alternating with expansion (wet season; Flügel 2004). As these cracks are filled with clay, it indicates illuvial processes typical of palaeosoils (Bhattacharyya and Chakraborty 2000).

MFO11b: mottled claystone

Clay is clearly dominant (>90%). Small grains of detrital quartz (≈0.1 mm) and mica sheets are also observed. Poorly preserved crinoids and brachiopods are rare. This claystone is coloured in red with greenish stains (Fig. 6m).

Interpretation. The abundance of detrital material combined to the particularly poor fauna indicates very proximal to supratidal settings. The mottling of the rock indicates variations of the oxydo-reduction state due to water-table fluctuations (Collinson 1996; Freytet and Verrecchia 2002) confirming the supratidal setting. Moreover, the association of mottled claystone and carbonate soils could indicate the development of an alluvial system (Sanz et al. 1995).

Summary of microfacies interpretation: palaeoenvironmental model

A palaeoenvironmental model is proposed (Fig. 7) to summarise and illustrate the interpretation of the microfacies types analysis. It corresponds to a complex ramp profile where calcareous-, siliciclastic- and mixed siliciclastic/calcareous deposits coexist. This model can be divided into four main sedimentary domains (Fig. 8).

1. The first domain (SD1) includes MFO1 and MFO2. It is located under the FWWB and corresponds to more distal settings, with important carbonate productivity and terrigenous input. The equilibrium between these two features allows the growing of metric-sized colonies of *Mesophyllum* and the development of a biostromal unit (related to unit iii).
2. The second domain (SD2) includes MFO4, MFO5, and MFO7. The first microfacies type is situated around the FWWB and the last two are located above. SD2 is characterised by the dominance of carbonate over detrital material. This suggests higher carbonate productivity and a relatively limited influence of terrigenous input when compared with the third domain.
3. This third domain (SD3) is laterally equivalent to SD2 and exposed to fair-weather waves. The terrigenous input is dominant, and the carbonate productivity relatively low. Microfacies MFO3, MFO6, MFO8, and MFO9 correspond to this SD3.
4. The SD4 domain encompasses intertidal to supratidal settings related to pedogenetic processes (MFO10 and MFO11).

Facies evolution

The microfacies evolution shows two general shallowing-upward trends (numbered A and B on Fig. 5a).

1. The first trend (41 m) corresponds to a slight deepening-upward (maybe related to the top of an incomplete trend) followed by a more marked shallowing-upward trend. The maximal bathymetry is associated with the base of the lower Nohn Formation. The top of this trend is assigned to very proximal settings (MFO8, MFO9, and MFO10).
2. The base of the second trend (from 41 to 92 m) is defined by a sharp transition from the trend before (MFO1–MFO8). Then, it corresponds to a shallowing-upward trend ending at the top of the section, with settings corresponding to MFO11a and MFO11b.

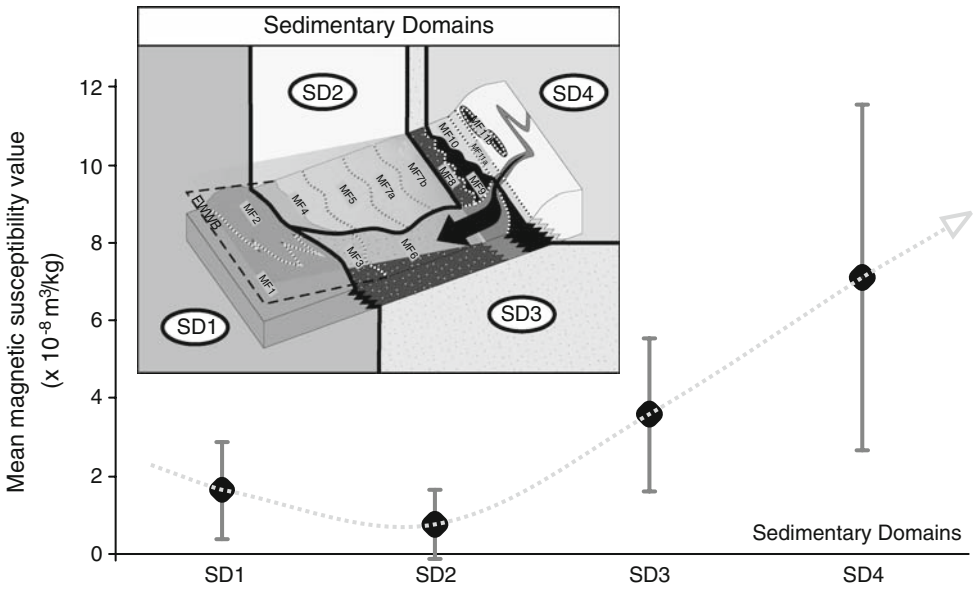

Fig. 8 Main magnetic susceptibility value for each sedimentary domain (numbered *SD1–SD4*) and evolution of this value along a distal-proximal scale)

Discussion

Comparison between microfacies and MS trends

Within the large-scaled shallowing trends recorded in facies evolution, four smaller successive trends (numbered I–IV on Fig. 5a) can be differentiated from MS. It is particularly interesting to compare microfacies and MS evolutions. Both curves show a well-marked parallelism between trends A and I (Fig. 5a). This parallelism is in agreement with the model of Crick et al. (1997), which predicts for each shallowing-upward trend a corresponding increase of the MS values. Deepening upward shows the opposite trend.

The situation for the microfacies trend B is more complicated. It comprises three successive MS trends (II–IV). The base of trend B is associated with low MS values and the top with high MS values, as predicted by the model of Crick et al. (1997); however, the middle part of the Dankerath Member (see Fig. 3 for stratigraphic position) is associated with unexpected high MS values (i.e., not linked to a fall in the sea level).

For a better understanding of the processes influencing MS variations at the Ohlesberg, the four main sedimentary domains (SD1–SD4) are envisaged and the average MS value is calculated. General increase of average MS value is observed from distal to proximal settings but not from SD1 to SD2 (Fig. 8). SD1 is characterised by a relatively low mean value of 1.62×10^{-8} m^3/kg as well as SD2 (0.75×10^{-8} m^3/kg). Values increase for SD3 (3.57×10^{-8} m^3/kg) and SD4 (7.12×10^{-8} m^3/kg). Although proximality appears to be the most important parameter on MS variations leading to higher MS values in SD4, carbonate productivity and wave agitation also seem to play a role.

The influence of carbonate productivity favours lower MS values than expected by diluting the MS carrying minerals (Mabille and Boulvain 2007b; da Silva et al. 2008). This is notably obvious for SD2 and SD3. Even if these two sedimentary domains are located in similar proximality, and are then supposed to be exposed to the same continental influence, SD2 shows lower MS values than SD3 because of higher carbonate productivity.

Moreover, wave agitation explains the slight lowering of mean MS value from SD1 to SD2. These two domains are both characterised by significant carbonate productivity. The increasing wave agitation is able to counterbalance the effect of increasing proximality on the MS values by preventing the settlement of small particles carrying the MS signals (Mabille and Boulvain 2007b).

This relatively intuitive approach explains the relationship between microfacies and MS evolution (MS trends from I to IV):

1. Decreasing MS values observed within the first MS trend corresponds to the transition from the top of the Lauch Formation dominated by SD3 to the base of the lower Nohn Formation characterised by SD1 and then SD2. The increasing of MS values observed in the upper part is related to the occurrence of microfacies belonging to SD3 and SD4.
2. Transition from lower to upper Nohn Formation corresponds to a shift from SD1 to SD3. This evolution is printed a general increase of SM values.
3. The third MS trend is associated with relatively low MS values due to the dominance of SD2 followed by higher values corresponding to SD3.
4. Within this last trend, minimal SM values are recorded on both sides of the boundary between Dankerath and Hundsell members. This is explained by the clear dominance of SD2 in this part of the section. Higher MS values are recorded at the base of the trend which is dominated by SD3 and near the top due to the occurrence of microfacies belonging to SD4.

The behaviour of MS depicted at the Ohlesberg indicates the interplay of at least three influencing parameters: the siliciclastic input, the dilution of this input by carbonate production and the wave agitation which is able to prevent the settlement of small particles carrying the MS.

Discussion of the Ohlesberg section in a regional context

The depositional setting described for the Ohlesberg section has to be placed in its regional context, firstly at the scale of the Sötenich Syncline and then within the Eifel area. The facies development at the Ohlesberg advocates for a ramp geometry in the depositional system (Fig. 7), but the spatial orientation of that ramp cannot be directly reconstructed from a single section. The integration of more data from other localities is required, but as already stated, data from the vicinity of the quarry are poor. Moreover, the scattered available data may not be characteristic in respect to the important spatial and temporal facies reported. Even though facies distribution of the Nohn Formation in the central Sötenich Syncline (Paulus 1959) advocates for a general dip towards the SE. The isopach map for the lower Nohn Formation (Fig. 9) does not show a conclusive image. A dip to the NW seems also be likely, especially due to the proximate position of the Ohlesberg section to the Mid-Eifelian High in its south. However, the complex facies distribution in the NE part of the Sötenich Syncline (Nowak 1956) greatly modifies this rather simple image.

At a larger scale, the isopach map for the lower Nohn Formation (Fig. 9) shows the existence of up to three depocenters. A SW–NE directed line which crosses the

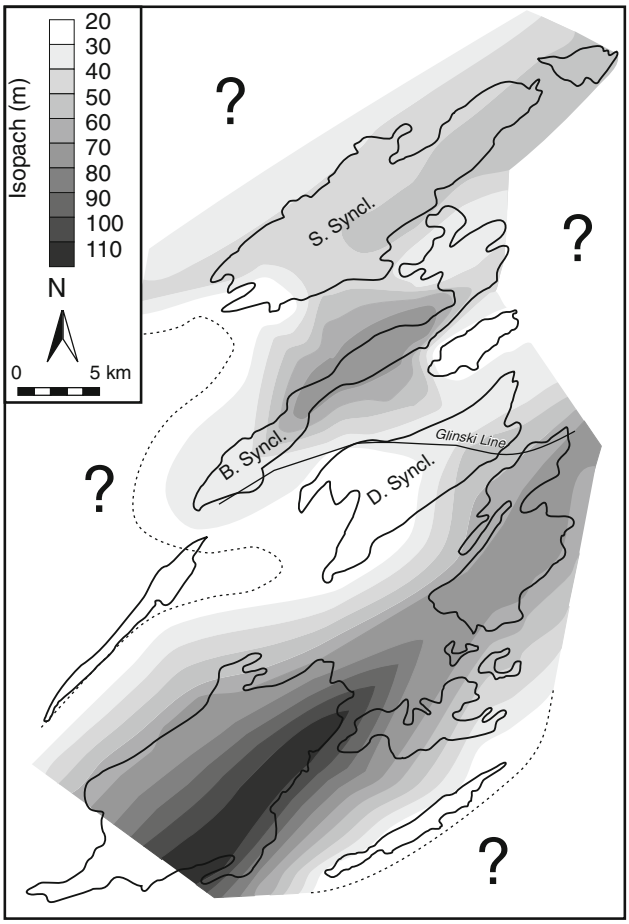

Fig. 9 Isopach map for lower Nohn Formation based on data in Meyer (1994). Since the thickness does not result from single sections, the map is based on areas and not on single points/localities, and thus shows the general trends and distributions, but may show for particular sections inappropriate values. Dollendorf Syncline (*D. Syncl*) separates the southern from the northern synclines. North of this separation delineated by the "*Glinski Line*" in the Junkerberg Formation, central Blankenheim Syncline (*B. Syncl*) and NE Sötenich Syncline (*S. Syncl*) correspond to the depocenter

Dollendorf Syncline clearly separates the southern from the northern synclines and implies an important break in the depositional environment for the entire Eifel synclines. This clear separation of the northern synclines from the southern is recorded in almost the same position in earlier times; "Glinksi Line" in the Junkerberg Fm (Middle Eifelian; for a discussion see Schröder 1998). In Nohnian times, the development of the eastern facies realm B (Fig. 1) cannot be deduced from the isopach data. North of the sharp separating line, the important reef system in the central Blankenheim Syncline is well delineated as one depocenter; the second depocenter in the NE Sötenich Syncline is characterised by less abrupt changes in thickness. However, based on this map and taking into account facies distribution, a simple SW–NE orientated spur (=Mid-Eifelian High) is difficult to constrain. The marked differentiation in that area might correspond to a ramp system with numerous topographic irregularities.

Discussion of lithostratigraphic units

The Ohlesberg section illustrates the complex facies mosaic of the Sötenich Syncline and adjacent synclines during the Lower Eifelian (Fig. 10). Fluctuations of sea level, carbonate productivity, siliciclastic influx, and deposition on a ramp are general characteristics for that time. A comparison of our results to available data in literature is particularly relevant.

Lauch Formation: Contrary to the general development of the Lauch Formation in the Eifel, where marly sediments and massive limestones with only few reefal organisms predominate, the lowest part of the exposed Ohlesberg section is remarkable for its comparably early onset of a weak reefal sedimentation. This may be seen as an initial phase of reef growth leading to the typical reefal units of the Lower Eifelian Nohn Formation.

Nohn Formation: The development of low-height stromatoporoid-dominated reefal units characterising the base of the lower Nohn Formation is a common phenomenon in the northern Eifel (Fig. 10). It corresponds to the "Stromtoporen Bankriffe" (e.g., Nowak 1956; Glinski 1961; Ochs and Wolfart 1961). However, differences exist for timing and individual sizes of these reefal units. In this regional frame, the Ohlesberg section is relatively atypical, because only one reefal unit is present. The relative scarceness of reef facies might be explained by a distal position in respect to the main reef development in the Zieverich area to the NE (Nowak 1956).

The development of solitary rugose corals, massive and laminar stromatoporoids, and colonies of fasciculate rugose corals (*Mesophyllum*) observed in the last third of the lower Nohn Formation might be contemporaneous to reefs in the lower part of the Schellgesberg Horizont (Paulus 1959) in the central part of the Sötenich Syncline (Nettersheim area). Following Paulus (1959), this reef-dominated facies continues from Nettersheim in north-eastern directions.

For the Nohn Formation, this time slice represents the peak in reef development in central and eastern parts of Sötenich and Blankenheim Synclines, and the entire Rohr Syncline (Fig. 10). A literature review shows that it is related to the volumetrically most important Nohnian reefs developed in the central Blankenheim Syncline (Ochs and Wolfart 1961) up to Kronenburg in the SW of that syncline (Schröder and Lütte 1999). This important reef development results in an increased thickness of the lower Nohn Formation in that area compared to the surroundings (Fig. 9).

The concentration of reefs on the southern limb of the Sötenich Syncline from Nettersheim to Kirchheim and in

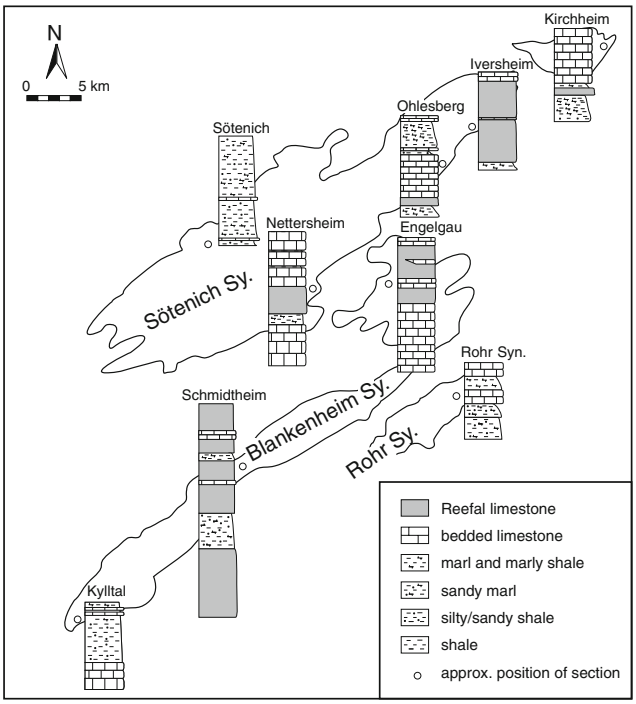

Fig. 10 Composite facies logs for several sections within the Sötenich, Blankenheim and Rohr synclines indicating the variable facies distributions in the lower Nohn Formation. Thickness and facies are based on the descriptions in Glinksi (1961), Meyer (1994), Nowak (1956), Ochs and Wolfart (1961) and Paulus (1959)

many parts of the Blankenheim Syncline (Fig. 10) can be related to the Mid-Eifelian High. The spatial and temporal variations of reef facies and its thickness indicate a reef belt along a topographic elevated structure, its SW extension would be larger than the normally postulated Mid-Eifelian High. This reef belt is complex and internally structured into reefal and non-reefal areas. The coeval variegated deposits of the eastern Blankenheim Syncline and Sötenich Syncline clearly show highly differentiated depositional environments on and along this high. The Ohlesberg section would be either in a distal position of the high or in a non-reefal area. However, all these environments belonged to the same major facies realm. The shelf break separating a more shallow northern and somewhat deeper southern facies realm, crosses further south the Dollendorf Syncline (Fig. 9).

The upper Nohn Formation of the Ohlesberg developed rather similar to the general patterns described by Rehfeld (1986). Concentrations of bioclasts in shell beds found in this part of the section are similar to the tempestite facies of Rehfeld. Also the presence of shallowing trends is a widespread phenomenon in that time slice. The third MS trend at the Ohlesberg in the middle of Dankerath Member can be parallelised with the "Karbonatische Zwischenfolge" of Klein et al. (1998), which represents an independent cycle indicating the fast sea-level fluctuations and important changes in the influx of siliciclastic material of that time.

The Hundsdell deposits correspond to a more uniform facies pattern for the northern Eifel synclines. This uniformisation might be due to less marked bathymetric differences within the area. However, formation of palaeosoils and fast changes in composition and thickness of individual beds indicate a high variability on the local scale, which hamper the correlation of single isochrons within the Hundsdell deposits. As it is impossible to estimate the lateral extension of palaeosoils observed at the top of section, they could either characterise a local emersion or have a regional significance linked to the presence of the Mid-Eifelian High.

Conclusion

Petrographic analyses of the Ohlesberg section led to the definition of eleven microfacies types representing a particularly complex ramp model. In this model, four sedimentary domains (SD) are defined. SD1 corresponds to the more distal settings observed (under FWWB). It is characterised by important carbonate productivity and terrigenous input. However, the equilibrium between these two features allows for the growing of metric-sized colonies of *Mesophyllum* and the installation of a biostromal unit (Stromatoporen Block-Riffe). SD2 differs from SD1 by an increase in wave agitation. This domain is defined by dominance of carbonate over siliciclastic material suggesting higher carbonate productivity and relatively limited influence of terrigenous input in comparison with the third domain. This SD3 represents the siliciclastic-dominated facies equivalent, which developed under similar hydrodynamical conditions. Terrigenous input dominates, and carbonate productivity is relatively low. Finally, SD4 encompasses intertidal to supratidal settings with the formation of palaeosoils.

The vertical succession of microfacies indicates a general shallowing upward trend. The base of the section corresponds to settings located around FWWB and the top is characterised by supratidal settings. This general trend is moreover divided into two successive shallowing-upward trends.

Magnetic susceptibility (MS) analyses coupled with microfacies analyses and interpretations domain by domain allows for the recognition of proximity as the main parameter responsible for MS variations. An increasing proximity to emerged areas leads to an increasing of MS values because of a greater influence of this source of MS carrying minerals. Additionally, two other MS controlling parameters are also noted: (1) carbonate productivity which is able to lower MS signal by diluting MS carrying minerals, and (2) water agitation possibly responsible for non-deposition of these MS carrying minerals.

The Ohlesberg section represents ramp environments in the vicinity of the Zieverich reef complex and can be well integrated into the facies mosaic of the NE Sötenich Syncline. The existence of the Mid-Eifelian High cannot be directly evidenced from this study, but if present, the basinal high was highly structured and surrounded and blanketed by very different facies.

Acknowledgements C. Mabille benefited from a FRIA grant from the Belgian Fond National de la Recherche Scientifique (FNRS). F. Boulvain acknowledges support through research grant FRFC 2-4501-02 (FNRS). A.-C. da Silva benefited from a Postdoctoral Researcher grant (FNRS). Two anonymous reviewers are deeply acknowledged for their numerous comments and remarks which greatly improved the paper.

References

Aigner T, Reineck H-E (1982) Proximality trends in modern storm sands from the Helegoland Bight (North Sea) and their implication for basin analysis. Senckenberg Marit 14:183–215

Bhattacharyya A, Chakraborty C (2000) Analysis of sedimentary successions: a field manual. Balkema, Rotterdam

Birenheide R (1978) Rugose Korallen des Devon. In: Krömmelbein K (ed) Leitfossilien begründet von Georg Gürich, Borntraeger, Berlin, 265 pp

Burchette TP, Wright VP (1992) Carbonate ramp depositional systems. Sediment Geol 79:3–57

Collinson JD (1996) Alluvial sediments. In: Reading HG (ed) Sedimentary environments: processes, facies and stratigraphy, 3rd edn. Blackwell, London, pp 37–82

Crick RE, Ellwood BB, El Hassani A (1994) Integration of biostratigraphy, magnetic susceptibility and relative sea-level change: a new look at high resolution correlation. Subcomm Dev Strat Newsl 11:35–66

Crick RE, Ellwood BB, El Hassani A, Feist R, Hladil J (1997) Magnetosusceptibility event and cyclostratigraphy (MSEC) of Eifelian-Givetian GSSP and associated boundary sequences in North Africa and Europe. Episodes 20:167–175

Crick RE, Ellwood BB, El Hassani A, Feist R (2000) Proposed magnetostratigraphy susceptibility magnetostratotype for the Eifelian-Givetian GSSP (Anti-Atlas, Morocco). Episodes 23:93–101

Dickfeld L (1969) Stratigraphie und Fazies im Westteil der Sötenicher Mulde (Devon/Eifel). PhD Thesis, Univ. Frankfurt/Main, Germany, 260 pp

Dunham RJ (1962) Classification of carbonate rocks according to depositional texture. Mem Am Assoc Pet Geol 1:108–121

Ellwood BB, Crick RE, El Hassani A (1999) The magneto-susceptibility event and cyclostratigraphy (MSEC) method used in geological correlation of Devonian rocks from Anti-Atlas Morocco. AAPG Bull 83:1119–1134

Ellwood BB, Crick RE, El Hassani A, Benoist SL, Young RH (2000) Magnetosusceptibility event and cyclostratigraphy method applied to marine rocks: detrital input versus carbonate productivity. Geology 28:1135–1138

Embry AF, Klovan J (1972) Absolute water depth limits of Late Devonian paleoecological zones. Geol Rundsch 61:672–686

Faber P (1980) Fazies-Gliederung und Entwicklung im Mittel-Devon der Eifel (Rheinisches Schiefergebirge). Mainzer Geowiss Mitt 8:83–149

Flügel E (2004) Microfacies of carbonate rocks: analysis, interpretation and application. Springer, Berlin

Freytet P, Verrecchia EP (2002) Lacustrine and palustrine carbonate petrography: an overview. J Paleolimnol 27:221–237

Glinski A (1961) Die Schichtenfolge der Rohrer Mulde. Senckenberg Leth 42:273–289

Goldfuss GA (1826) Abbildungen und Beschreibungen der Petrefacten Deutschlands und der angrenzenden Länder. Erster Theil. I-VIII, Arnz, Dusseldorf, Germany, pp 1–252

Happel L, Reuling HT (1937) Die Geologie der Prümer Mulde. Abh Senckenberg Naturff Ges 438:1–94

Hladil J (1992) Are there turbidites in the Silurian/Devonian Boundary Stratotype? Klonk near Suchomastry, Barrandian, Czechoslovakia. Facies 26:35–54

Hladil J (2002) Geophysical records of dispersed weathering products on the Frasnian carbonate platform and Early Famennian ramps in Moravia, Czech Republic: proxies for eustasy and palaeoclimate. Palaeogeogr Palaeoclimatol Palaeoecol 181:213–250

Howard JD, Reineck H-E (1981) Depositional facies of high-energy beach-to-offshore sequence: comparison with low-energy sequence. AAPG Bull 65:807–830

Johnson HD, Baldwin CT (1996) Shallow clastic seas. In: Reading HG (eds) Sedimentary environments: processes, facies and stratigraphy, 3rd edn. Blackwell, London, pp 232–280

Kershaw S (1998) The applications of stromatoporoid palaeobiology in palaeoenvironmental analysis. Palaeontology 41:509–544

Kershaw S, Brunton FR (1999) Palaeozoic stromatoporoid taphonomy: ecologic and environmental significance. Palaeogeogr Palaeoclimatol Palaeoecol 149:313–328

Klein H, Utescher T, Langer W (1998) Zur Karbonatmikrofazies der unteren Eifel-Stufe/Mitteldevon am Ohlesberg bei Bad Münstereifel/Eifel. Decheniana 151:227–243

Krömmelbein K, Hotz E-E, Kräusel W, Struve W (1955) Zur Geologie der Eifeler Kalkmulden. Beih Geol Jb 17:45–192

Kumar N, Sanders JE (1976) Characteristics of shoreface storm deposits: modern and ancient examples. J Sediment Pet 46:145–162

Mabille C, Boulvain F (2007a) Sedimentology and magnetic susceptibility of the Upper Eifelian—Lower Givetian (Middle Devonian) in southwestern Belgium: insights into carbonate platform initiation. In: Alvaro JJ, Aretz M, Boulvain F, Munnecke A, Vachard D, Vennin E (eds) Palaeozoic reefs and bioaccumulations: climatic and evolutionary controls. Geol Soc London Spec Publ 275:109–123

Mabille C, Boulvain F (2007b) Sedimentology and magnetic susceptibility of the Couvin Formation (Eifelian, south western Belgium): carbonate platform initiation in a hostile world. Geol Belgica 10(1–2):47–68

Mabille C, Boulvain F (2008) Les Monts de Baileux section: detailed sedimentology and magnetic susceptibility of Hanonet, Trois-Fontaines and Terres d'Haurs formations (Eifelian/Givetian boundary and lower Givetian, SW Belgium). Geol Belgica 11:93–121

Meyer W (1994) Geologie der Eifel. Schweizerbart, Stuttgart, Germany

Monty C (1967) Distribution and structure of recent stromatolitic algal mats, Eastern Andros Island, Bahamas. Ann Soc Géol Belgique 90:55–100

Nowak HJ (1956) Stratigraphische Untersuchungen im nordöstlichen Abschnitt der Sötenicher Mitteldevonmulde (Eifel). Decheniana 2:1–68

Ochs G, Wolfart R (1961) Geologie der Blankenheimer Mulde (Devon, Eifel). Abh Senckenberg Naturfr Ges 501:1–100

Paulus B (1959) Der mittlere Teil der Sötenicher Mulde (Devon, Eifel) I. Unterdevon und tiefes Eifelium. Senckenberg Leth 40:333–365

Paulus B (1961) Der mittlere Teil der Sötenicher Mulde (Devon, Eifel) II. Nachträge und das höhere Eifelium. Senckenberg Leth 42:411–452

Pettijohn FJ, Potter PN, Siever R (1972) Sand and sandstone. Springer, Berlin

Préat A, Kasimi R (1995) Sédimentation de rampe mixte silico-carbonatée des couches de transition eifeliennes-givetiennes franco-belges. Première partie: microfaciès et modèle sédimentaire. Bull Cent Rech Explo-Produc Elf Aquitaine 19:329–375

Rehfeld (1986) Die Tempestitfazies in den Oberen Nohner Schichten (Unteres Mitteldevon) der Eifel (Linksrheinisches Schiefergebirge). Neues Jahrb Geol Paläontol 11:681–703

Sanz ME, Alonso Zarza AM, Calvo JP (1995) Carbonate pond deposits related to semi-arid alluvial systems: examples from the Tertiary Madrid Basin, Spain. Sedimentology 42:437–452

Schlüter C (1889) Anthozoen des rheinischen Mittel-Devon. Abh Geol Spezialkarte Preussen u Thüring Staaten, Königl Preuß Geol L-A 8:1–207

Schröder S (1998) Rugose Korallen und Stratigraphie des oberen Eifelium und unteren Givetium der Dollendorfer Mulde/Eifel (Mittel-Devon; Rheinisches Schiefergebirge). Cour Forsch Inst Senckenberg 208:1–135

Schröder S, Lütte B-P (1999) Über den taxonomischen Status von "*Fasciphyllum varium Schlüter* 1889" (Rugosa/Mittel-Devon der Eifel). Senckenberg Leth 79:119–129

Sepkoski JJ Jr, Bambach RK, Droser ML (1991) Secular changes in Phanerozoic event bedding and biological overprint. In: Einsele G, Ricken W, Seilacher A (eds) Cycles and events in stratigraphy. Springer, Berlin, pp 298–312

da Silva AC, Boulvain F (2006) Upper Devonian carbonate platform correlations and sea level variations recorded in magnetic susceptibility. Palaeogeogr Palaeoclimatol Palaeoecol 240:373–388

da Silva AC, Potma K, Weissenberg JAW, Whalen MT, Humblet M, Mabille C, Boulvain F (2008) Magnetic susceptibility evolution and sedimentary environments on carbonate platform sediments and atolls, comparison of the Frasnian from Belgium and from Alberta, Canada. Sediment Geol (in press)

Stage M (2001) Magnetic susceptibility as carrier of a climatic signal in chalk. Earth Planet Sci Lett 188:17–27

Steiniger J (1853) Geognostische Beschreibung der Eifel. Lintzsche, Trier, Germany

Struve W (1963) Das Korallen-Meer der Eifel vor 300 Millionen Jahren: Fund, Deutungen, Probleme. Nat Mus 93:237–276

Struve W (1982) The Eifelian within the Devonian frame, history, boundaries, definitions. Cour Forsch Inst Senckenberg 55:401–432

Tucker ME, Wright VP (1990) Carbonate sedimentology. Blackwell, London

Winter J (1977) Exkursionsbericht- Geologische Exkursion in den Raum Weyer-Schuld-Heyroth-Niederehe-Üxheim-Ahütte. Decheniana 130:322–334

Wright VP (1994) Paleosoils in shallow marine carbonate sequences. Earth Sci Rev 35:367–395

Wright VP, Burchette TP (1996) Shallow-water carbonate environments. In: Reading HG (ed.) Sedimentary environments: processes, facies and stratigraphy, 3rd edn. Blackwell, London, pp 325–394